Mechanical characterization of individual polycrystalline carbon tubes for use in electrical nano-interconnects

A. Khiat [a,*], R.H. Poelma [b], G.Q. Zhang [b,c], F. Heuck [a], F.D. Tichelaar [d], M. Sarno [e,f], P. Ciambelli [e,f], S. Fontorbes [g], L. Arurault [g], U. Staufer [a]

[a] *Precision and Microsystems Engineering, Delft University of Technology, Delft, The Netherlands*
[b] *DIMES Centre for SSL Technologies, Delft University of Technology, Delft, The Netherlands*
[c] *Philips Lighting Laboratory, Philips, Eindhoven, The Netherlands*
[d] *National Centre for HREM, Kavli Institute of Nanoscience, Delft, The Netherlands*
[e] *Università degli Studi di Salerno, Dipartimento di Ingegneria Chimica e Alimentare, Fisciano(SA), Italy*
[f] *NANO_MATES, Research Centre for Nanomaterials and Nanotechnology at University of Salerno, Fisciano(SA), Italy*
[g] *Université de Toulouse, CIRIMAT, UPS/INPT/CNRS, Toulouse, France*

ARTICLE INFO

Keywords:
Polycrystalline carbon tubes
CVD growth
CNT without catalyst
Mechanical characterization
Electrostatic pull-in measurement

ABSTRACT

Polycrystalline carbon tubes were generated by CVD inside electrochemically prepared nano-porous anodic aluminium oxide membranes. This method produced nano-tubes without catalyst, featuring polycrystalline and a few layer thick walls. Individual tubes could be isolated and suspended on microfabricated substrates such that they formed single-side clamped beams. These beams were then used to investigate their mechanical properties employing electrostatic forces for bending the tubes beyond their mechanical stability where pull-in occurs, which could be detected by monitoring the current flowing from the tube to the substrate.

1. Introduction

The exceptional mechanical, thermal and electrical properties of Carbon nano-tubes (CNTs) are the main motivations for many research activities in nanotechnology. Microelectronic devices, electrochemical probes, intramolecular gene delivery devices, scanning probe microscopy tips, nanoporous membranes, composite materials, Hydrogen and energy storage [1,2] are some applications, which aim taking advantage of the properties of CNTs. Knowing the exact mechanical properties of the employed CNTs is important to predict the reliability and the functionality of these elements.

Since their discovery, it was expected that CNTs would display extraordinary mechanical properties [3]. Long before sufficient quantities of CNTs were produced to allow mechanical measurements, a number of studies had used computer simulation to study and predict their properties [4] calculating a Young's modulus of 1.5 TPa, similar to the value for an individual graphite layer. This study was followed by papers predicting that the Young's modulus of CNTs was close to 1 TPa independent of CNT type and diameter [5]. Different methods have been used to investigate the Young's modulus of CNT. Two studies from Enomoto et al. [6] and Masahiro et al. [7] used a nano-probe manipulator fitted into a transmission electron microscope to mechanically manipulate the CNT. In the studies of Arun et al. [8], the Young's modulus of a CNT was determined by electrostatically manipulating several carbon nano-tubes (forest) simultaneously and Salvetat et al. had used the AFM technique to bend the tubes [9]. They had measured Young's moduli between 12 and 50 GPa.

In the presented study, which is part of the European project *Catherine* [10], polycrystalline carbon tubes were generated and investigated for potential applications in the next generation high speed electrical nano inter-connection. Here, the technology to generate those carbon tubes was presented and The Young's moduli were determined by the electrostatic pull-in instability method proposed initially by Sadeghian et al. [11] for MEMS (silicon cantilevers), which was further advanced here for NEMS (investigating individual nanometre sized nano-tubes). This method was chosen because its implementation is easy for the nano-elements, it's robust, repeatable, high accurate. The experiments were done outside SEM or TEM to avoid any damage of the specific carbon nano-tubes with the electron beam.

2. Methods

Carbon tubes were synthesized by CVD into a template [2]. We used Ethene (C_2H_4) as precursor and nano-porous Anodic Aluminium Oxide [AAO] membrane without catalyst as template.

* Corresponding author.
E-mail address: a.khiat@imperial.ac.uk (A. Khiat).

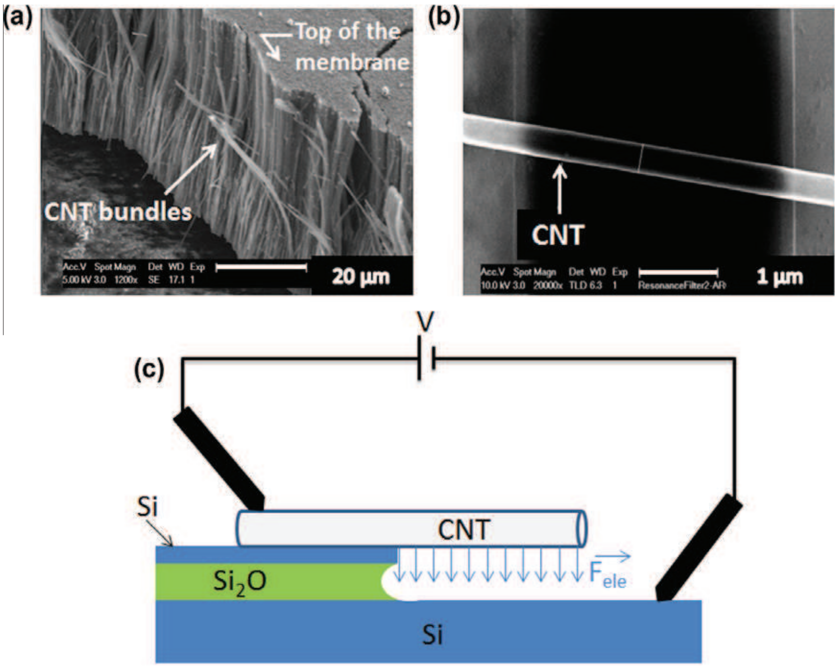

Fig. 1. (a) Nano-porous AAO membrane with carbon tubes, (b) extracted carbon tube, (c) principle of the experiment.

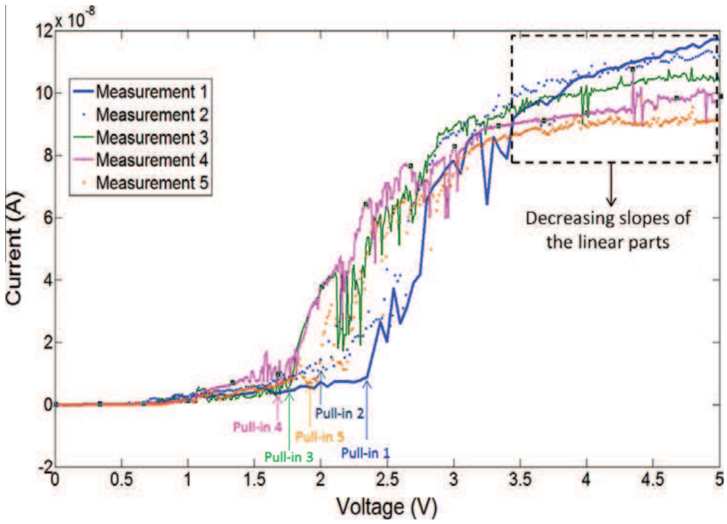

Fig. 2. Voltage–current measurement curves (L = 13.6 µm).

The membranes had a diameter of 1 cm, a thickness of 60 µm and the average pore diameter was 365 ± 10 nm. The deposition time was 20 min under isothermal conditions after a pre-treatment of the membrane under nitrogen flow from room temperature up to 970 °C. The flow rate was 200 Ncc/min of C_2H_4 3% v/v in N_2. The gas flows were arranged to be vertical for better controlling the fluid dynamics of the reactor, forcing the flow to pass through the membrane. The result is shown in Fig. 1a.

To individualize nano-tubes, nitrogen (N_2) plasma was used to sputter-etch a non-desirable carbon layer, which grew during the CVD on the top and bottom surfaces of the membrane. The optimum etching was obtained at N_2 flow rate of 60 sccm, pressure of 0.015 mbar and power of 100 Watt. The AAO membrane was then selectively removed by wet-etching for 5 min in 0.5 M sodium hydroxide (NaOH) resulting on bundles of tubes, which were suspended in ethanol then sonicated for 20 min to obtain individual tubes. The sonication time is a critical trade-off between sufficiently separating the bundles and damaging individual tubes.

The substrate featuring the electrodes for the pull-in experiments was microfabricated from a silicon-on-insulator (SOI) wafer. The base silicon layer was 500 µm, the buried, isolating silicon dioxide 1019 nm, and the device layer 340 nm thick. The device and insulating layer were locally etched to form a step (Fig. 1c).

A small droplet of ethanol containing suspended tubes was dispensed on the substrate. After evaporation some tubes were found as freestanding cantilevers, which were attached on one side to the device layer and hanged over the base layer with their free end (Fig. 1c). SEM images allowed measuring the average nano-tube diameter, 365 ± 5 nm, which is equal to the pore diameter. These images were taken on tubes that were not used for the experiments afterwards, avoiding possible errors by e-beam induced damages.

The Young's moduli, E, of individual nano-tubes were measured based on an electrostatic pull-in experiment [11]. The chip with the suspended nano-tubes was mounted in a prober station (Mod. XY Süss Microtec). The top electrode and the nano-tube were contacted by placing a probe needle onto the nano-tubes, while the bottom electrode was contacted with a second probe. The surface underneath the probe needles was scratched to remove any possible oxide layer and to ensure good electrical contact. Both probes were then connected to a source measure unit (Keithley 2600), which in turn was connected to a data acquisition system.

3. Experiments

Applying and increasing a voltage, V, between the two electrodes caused the nano-tube to bend towards the base layer because of the electrostatic force. The magnitude of this force was a strong function of the applied voltage and of the distance between the cantilever and the substrate, x. At a certain voltage, which is called the pull-in voltage, the electrostatic forces become stronger than the mechanical strength of the nano-tube. The system became instable and the free end snapped to the base layer. This was monitored by measuring the current, J.

An example of the measurements realized is shown in Fig. 2 were the same experiment was repeated five times by increasing the voltage from 0 to 5 V. In the first part of the curves, the current was very low (pA range) because the nano-tube cantilever was far from the substrate ($d_0 = 1359 \pm 10$ nm). At a specific bias, we observe a suddenly a sharp increasing of the current with a big slope. In this part of the curve, the nano-tube cantilever became unstable and snapped down to the substrate. The beginning of these disturbances was identified as pull-in voltage. In the last part of the curve, the current increased linearly but with much smaller slope. This was interpreted that the nano-tube was in contact with the substrate and the whole system was in a mechanically stable position, while the slope represented the ohmic contact between the device and base layer through the nano-tube.

When the voltage was set back to zero, the nano-tube cantilever was retracted. We waited for few minutes to eliminate any remained electrostatic charges, we observe that the current dropped to zero, then the experiment was started again using the same nano-tube cantilever (Fig. 2). The polycrystalline carbon tubes used in this experiment are large compared to pristine CNTs size, which allow us observing the CNT's pull-in and retraction (when the voltage is set at zero) under an optical microscope. This observation proves the mechanical aspect (pull-in) of this experiment. The experiment was done on different CNTs and the results are shown in Table 1.

The general characteristic was comparable to the first experiment but there were significant differences on the pull-in voltage value and on the final linear part. Generally, the pull-in voltage was lower for each consecutive experiment and also the slope of the linear part became smaller, which means that the electrical conductivity had decreased. After several repetitions the CNT stick to the surface and acts as a conductive wire.

Table 1
Young's modulus.

Tube	Exp. No.	L (μm)	V_{PI} (V)	E (GPa)	Uncertainty (GPa)
1	1	13.6	2.45	**1.02**	**±0.11**
1	2	13.6	2.06	0.73	
1	3	13.6	1.79	0.55	
1	4	13.6	1.59	0.43	
1	5	13.6	1.84	0.58	
2	1	17.4	1.54	**1.07**	**±0.08**
2	2	17.4	1.41	0.9	
2	3	17.4	1.37	0.85	
3	1	8.9	5.75	**1.07**	**±0.18**
3	2	8.9	4.9	0.78	
3	3	8.9	5.05	0.83	
3	4	8.9	5.09	0.84	
4	1	10.4	4.17	**1.04**	**±0.15**
4	2	10.4	4.59	1.25	
4	3	10.4	2.77	0.46	
4	4	10.4	2.69	0.43	
5	1	8.1	6.79	**1.03**	**±0.20**
6	1	8.9	5.59	**1.01**	**±0.17**
7	1	8.5	6.4	**1.11**	**±0.20**
8	1	9	5 .87	**1.17**	**±0.20**
9	1	8.7	6	**1.07**	**±0.19**

4. Data analysis

An analytical model was developed based on the study of J.A. Weldon [12], where electrostatic and mechanical forces applied on the nano-tube were given. The electrostatic force has two components, electrostatic sidewall force (F_s) which is a distributed force and an electrostatic force acting on the nano-tube tip (F_t):

$$F_s(x,V) = \frac{\pi\varepsilon_0 L}{\sqrt{(d_0 - \frac{x}{2})((d_0 - \frac{x}{2}) + 2r)} \arccos h^2\left(1 + \frac{d_0 - \frac{x}{2}}{r}\right)} V^2 \quad (1)$$

$$F_t(x,V) = \frac{0.85\pi\varepsilon_0((d_0 + r)^2 r)^{1/3}}{\sqrt{(d_0 - x)((d_0 - x) + 2r} \arccos h^2\left(1 + \frac{d_0 - x}{r}\right)} V^2 \quad (2)$$

where, r is the nano-tube outer radius, ε_0 is the permittivity of vacuum. The elastic response of the nano-tube is represented by the spring constant which is given by two components, nano-tube sidewall and nano-tube tip spring constants:

$$k_s = \frac{8EI}{L^3}, k_t = \frac{3EI}{L^3} \quad (3)$$

where, I is the CNT moment of inertia. The model was adapted to the measured pull-in voltage by adjusting the Young's modulus of the nano-tube. High resolution transmission electron microscope (HR-TEM) images were used to measure the wall-thickness of the nano-tube, which was found to be equal to 5 nm. This gives an outer diameter, D_O, of 365 nm and an inner diameter, D_i, of 355 nm. A plot of the total force based on the sum of the electrostatic forces and an effective spring constants (k_s, k_t) as function of the tip – substrate distance is shown in Fig. 3. The direction of electrostatic force is considered to be positive. In order to find the right Young's modulus of the nano-tube, we took the voltage for which pull-in was observed. Pull-in is characterized by the fact that there is only

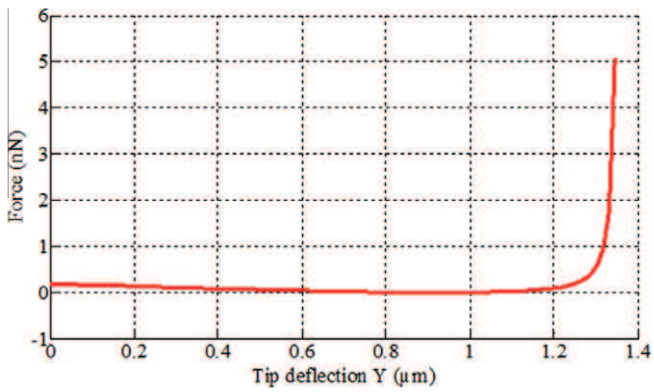

Fig. 3. Real curve corresponding to a Young's modulus of 1.02 GPa (L = 13.6 μm).

Fig. 4. (a) HR-TEM of carbon tube structures, (b) FFT image shows carbon tube graphite like spacing.

one gap distance where the total force is equal to zero (the instable position). The Young's modulus of the nano-tube is then equal to the one which has a horizontal tangent at its root.

It's interesting to observe that it was difficult to repeat the experiment for a single nano-tube: By conducting the pull-in experiment several times with the same nano-tube, the pull-in voltage was found generally to decrease, thus the Young's modulus, as shown in Table 1. This could be caused by the electrostatic charges remaining, after each experiment, between the nano-tube and the substrate. But, few minutes were used between the measurements to minimize the charging effect and the possibility of observing the pull-in effect under an optical microscope allow us to interpret this phenomenon rather as sign for a modification of the mechanical characteristics of the specific nano-tubes used in this project: The stiffness of the nano-tube became weaker after each experiment which changes the initial gap (d_0). Fig. 2 strengthens this interpretation, where the linear parts of the curves for sample 1 are shown; the slope is decreasing after each repetition, indicating an increasing resistance. This could be due to an increasing amount of structural defects. We therefore concluded that only the first measurement for each nano-tube should be used for extracting the Young's moduli.

The uncertainties are also calculated considering, in the developed model, different tolerances of the nano-tube length, diameter, pull-in voltage and the gap nano-tube / substrate, for which we found an average E of 1.07 ± 0.16 GPa.

From the HREM and fast Fourier transform, FFT, images shown in Fig. 4a and b, we observe that the wall structure of the nano-tubes consists of graphite like structures of 3.5 ± 0.2 Å spacing and amorphous carbon. This figure shows that the wall structure of the used carbon nano-tubes is not similar to a pristine multi walled CNT structure. The layers of the used tubes are more disordered, therefore their structure changes even after a small bending of the nano-tube.

5. Summary and conclusion

Novel carbon nano-tubes were generated by CVD into porous anodized aluminium oxide. This template synthesis permits to obtain open-end nano-tubes, with diameters that can reach hundreds of nanometres, a well-controlled central canal and high purity. However, the tubes were not crystalline but rather showed only partially ordered graphitic patches and amorphous carbon, a thermal annealing (>2000 °C) would be required to improve the structure. The mechanical properties of these tubes were analysed by electrostatic pull-in experiments. The results revealed a Young's modulus of 1.07 ± 0.16 GPa.

Acknowledgments

This work was supported by EU FP7 project, called Catherine, G.A. n. 216215.

References

[1] A.V. Melechko, V.I. Merkulov, T.E. McKnight, M.A. Guillorn, K.L. Klein, D.H. Lowndes, M.L. Simpson, J. Appl. Phys. 97 (2005) 041301.
[2] P. Ciambelli, L. Arurault, M. Sarno, S. Fontorbes, C. Leone, L. Datas, D. Sannino, P. Lenormand, S. Le Blond Du Plouy, NanoTechnology 22 (2011) 265613.
[3] J.N. Coleman, U. Khan, W.J. Blau, Y.K. Gun'ko, Carbon 44 (9) (2006) 1624–1652.
[4] G. Overney, W. Zhong, D. Tomanek, Zeitschrift Fur Physik D-Atoms Molecules and Clusters 27 (1993) 93–96.
[5] J.P. Lu, J. Phys. Chem. Solids 58 (1997) 1649–1652.
[6] K. Enomoto, S. Kitakata, T. Yasuhara, N. Ohtake, T. Kuzumaki, Y. Mitsuda, Appl. Phys. Lett. 88 (2006) 153115.
[7] M. Nakajima, F. Arai, T. Fukuda, IEEE Trans. Nanotechnol. 5 (2006) 243–248.
[8] A. Arun, D. Acquaviva, M. Fernández-Bolaños, P. Salet, H. Le-Poche, P. Pantigny, T. Idda, A.M. Ionescu, Microelectron. Eng. 87 (2010) 1281–1283.
[9] J.P. Salvetat, A.J. Kulik, J.M. Bonard, G.A.D. Briggs, T. Stockli, K. Metenier, S. Bonnamy, F. Beguin, N.A. Burnham, L. Forro, Adv. Mater. 11 (1999) 161–165.
[10] www.catherineproject.eu.
[11] H. Sadeghian, C.K. Yang, J.F.L. Goosen, E. van der Drift, A. Bossche, P.J. French, F. van Keulen, Appl. Phys. Lett. 94 (2009) 221903.
[12] J.A. Weldon, B. Alemán, A. Sussman, W. Gannett, A.K. Zettl, Nano Lett. 10 (5) (2010) 1728–1733.